Exploremetics
Journal of Innovative
Engineering and Technology

Volume: 02 No: 01 | March -2018

ISSN (Online) 2636 – 590
ISSN (Print) 2636 - 591X

OPTIMIZATION OF THE ADSORPTION OF IRON FROM AQUEOUS SOLUTION USING CASSAVA BAGASSE

CHIME Thompson Onyejiuwa [1], OSEKWU Emmanuel [2], ONOH Ikechukwu Maxwell [3]

1,2 and 3 Chemical Engineering Department, Enugu State University of Science and Technology, (ESUT) Enugu, Nigeria.

Email address: maxcalab001@gmail.com

Abstract - Heavy metals rank as major environmental pollutants. This study was carried out to optimize the efficiency of iron removal from an aqueous solution using chemically activated cassava bagasse as adsorbents. Process factors such as time, temperature, pH, dosage and initial metal concentration were investigated to optimize the adsorption process. Central Composite Rotatable Design (CCRD) of Response Surface Methodology (RSM) which produced 50 runs was employed for this optimization studies. The ANOVA result of the optimization study showed that both model and process parameters investigated were significant as their individual F-values were significant and their p–value <0.005. Optimization model equation was also obtained for the adsorption processes. From Numerical solution generated by the Design expert software, the optimum conditions for iron adsorption using cassava bagasse are: 86.14 minutes, 64.65°C, pH of 7.47, 0.24 g/30ml adsorbent dosage, initial metal concentration of 139.35 mg/l and 98.23% removal. The predicted, actual and adjusted coefficients of determination R^2 values are 0.991, 0.998 and 0.996 respectively. These R^2 values implied that the data fit the quadratic model and suggest an excellent correlation between the independent variables. A relatively low value of coefficient of variation (CV=8.9%) indicates a good precision and reliability of the experiments carried out.

KEYWORD: Cassava bagasse, Iron, Optimization, CCRD, Adsorption

1.0 INTRODUCTION

Presence of heavy metals in water as contaminants is an indication of global industrialisation attributed to large scale of inappropriate disposal and treatment of wastewater containing heavy metal from anthropogenic sources (United Nations Commission on Sustainable Development, 2010). Rapid acceleration of industrial growth throughout the world exerts negative impacts on the environment. Discharge of contaminated effluents without adequate treatment into the aquatic environment creates such implication. Industrial wastewater which are associated with manufacturing of automobile, purification of metals, electroplating, galvanizing, coating, paint, electronics, pharmaceutical, chemicals and battery manufacturing are the most common sources of heavy metal pollution. Arsenic, cadmium, copper, chromium, lead, mercury, nickel and zinc are normally found in heavy metal contaminated wastewater (Trueby, 2003).

Heavy metals such as iron, cadmium, lead and nickel exhibit toxic and persistent characteristics which can affect living organisms and the environment. Heavy metals naturally enter the human body through ingestion, inhalation and adsorption in small extent as trace elements. Trace elements are essential to maintain the metabolism of human body. However, trace amount of heavy metals

are dangerous because they tend to bio-accumulate and bio-magnify. Bio-accumulation and bio-magnification increase the concentration of heavy metal in a biological organism or targeted organ(s) over time until they become hazardous to health (Gupta et al., 2015). Acute exposure to high concentration of heavy metal can cause nausea, anorexia, vomiting, gastrointestinal abnormalities and dermatitis. From the perspective of human health, each of the heavy metals impact has different effects and symptoms (Sarkar et al., 2003). Therefore, the need to manage the amount of heavy metals released into the environment.

Agricultural waste materials are now becoming viable alternatives since they are predominantly available, cheaper and have various functional groups such as carboxylic acid, ester, carboxylate, hydroxyl, phenolic and amino groups that can act as adsorption sites for heavy metal ions (Ngah, 2007). Nigeria is one of the world's leading producers of cassava for alcohol industries. Cassava processing industries produce large amount of cassava bagasse which is cellulose material and can be used as low-cost biomass for the adsorption of total dissolved solids (TDS) (Osvaldo et al., 2007). The aim of this work, is to optimize the performance of cassava bagasse as a material for adsorption of iron from aqueous solution by chemically activating it using phosphoric acid.

2.0 MATERIALS AND METHODS

2.1 Materials

Cassava bagasse (CB) was obtained from a local cassava processing site in Enugu metropolis, Nigeria. The collected cassava bagasse was manually screened for stones and sands, and thereafter washed to remove dirt. It was further oven dried at 105˚C for 4 hours. The dried cassava bagasse was ground using electric blender and packed in polyethylene bags.

2.2 Methods

The cassava bagasse was characterized by proximate analysis, using standard methods of analysis for moisture, volatile matter, ash, and fixed carbon contents (AOAC, 1990). The structural/morphological analysis was done using scanning electron microscopy (SEM), while the functional groups present were ascertained using Fourier transform infrared (FTIR).

A sample of the cassava bagasse (CB) was thermally activated by heating in a muffle furnace at 800°C for 4 hours, cooled and chemically activated by soaking in 2M solution of phosphoric acid. The treated CB was washed using distilled water until a neutral pH was obtained. A second carbonization process was then carried out at 600°C for 4 hours, after which they were allowed to cool. The activated carbon was tightly sealed to prevent absorption of moisture.

Aqueous solution of iron (stock solution) was prepared from ferrous ammonium sulfate by dissolving 5.07g of ferrous ammonium sulfate in 1000ml of distilled water. The working solutions of various concentrations (standard solutions) were prepared by appropriately diluting the stock solution.

2.3 Adsorption and Optimization Study

The adsorption experiment was carried out by batch technique. The matrix table for the optimization study was designed using the Central Composite Rotatable Design (CCRD) of Response Surface Methodology (RSM) as shown in Table 2.1.

The adsorption experiment was carried out in batch process. Known initial metal concentrations(C_o) of each of the stock solutions were prepared, measured and poured into plastic bottles. The plastic bottles were capped tightly to avoid any leakage and placed in water baths. A certain dosage of the adsorbent was measured and added to the solution. The mixture was agitated at a constant speed of 200rpm and allowed to attain a particular temperature for a certain period of time according to the design of the experiment (DOE) When the contact time elapsed, the solution was filtered into different plastic bottles using filter paper. The final concentration (C_e) was measured using Atomic Absorption Spectrophotometer (AAS) and recorded against the design run in a separate column. The atomization of the sample in the AAS machine was achieved using a mixture of

acetylene and air as the energy source. The machine was standardized using iron standard obtained from Bulk Scientific, the manufacturers of the machine. The wave length of the machine was set at 560 nm for iron analysis. The absorption energy was supplied through hollow cathode lamps. The lamp was designed for the iron. The experiment was done by varying the process parameters as shown in Table 2.1 below.

Table 2.1: Factors and levels for the optimization

Variable	Symbol	Coded Variable Levels		
		-1	0	+1
Time(minute)	A	40	65	90
Temperature (˚C)	B	50	60	70
pH	C	5	7.5	10
Dosage (g)	D	0.1	0.2	0.3
Initial metal Conc. (mg/l)	E	75	112.5	150

3.0. RESULTS AND DISCUSSIONS

3.1 Characterization Studies

The proximate composition of raw and activated cassava bagasse is presented in Table 3.1. After carbonization and activation, the % fixed carbon content of the cassava bagasse (CB) increased significantly while the % ash and volatile matter content reduced drastically.

Table 3.1: The proximate composition of cassava bagasse

Component	Raw Cassava bagasse	Activated Cassava bagasse
Moisture content %	6.0	1.3
Volatile matter %	90.4	21.3
Ash content %	1.2	0.4
Fixed carbon %	2.4	12.2

FTIR analysis of the raw and carbonized cassava bagasse are presented in Table 3.2. From Table 3.2, it is observed that carbonization of the cassava bagasse removed some functional groups. The wide gap O-H stretch was observed to be narrow showing that some volatile matters were removed. It was also observed that after carbonization the major functional groups are O-H, -CH-,C = C – C, C = O.

Table 3.2: FTIR of raw and carbonized cassava bagasse

Raw Cassava Bagasse	Assignment	Carbonized Cassava Bagasse
Frequency (cm^{-1})	Assignment	Frequency (cm^{-1})
3682.057	O-H stretch	3667.105 - 3828.552
-	Hydroxyl group, H-bonded, O-H stretch	3592.012
3417.071	NH stretch	3457.103
3161.267	Aliphatic secondary amine, NH stretch	3161.388 - 3269.187
2833.277-3009.353	Normal “polymeric” OH stretch	2888.185 - 3019.095
2719.18	Methylamino, N-CH3, C-H stretch	2751.351
2458.03 - 2510.153	Isocynanate (-N=C=O asym. Stretch)	2450.146 – 2601.215
2121.222	Cynaide ion, thiocynanate ion and related ions	2145.998 – 2270.781
1998.105	Aromatic combination	1974.948
-	Conjugated ketone -C=O, open-chain acid anhydride	1857.628
1610.584, 1697.173	C=C-C Aromatic ring stretch	1630.752
1453.226	O-H bend	-
1322.655	N-O asymmetric stretch	1374.225
-	Aromatic C-H in plane bend	1277.913
-	Cyclohexane ring vibrations, Methyne - **CH–)**	1106.068
806.0274	Peroxides, C-O-O- stretch	841.1585
779.48	C-Cl stretch, Alkyne C-H bend	767.8679

Table 3.2: FTIR of raw and carbonized cassava bagasse

Type of Assignment or Functional Group	Raw Cassava Bagasse (Frequency)	Carbonized Cassava Bagasse (Frequency)
O-H stretch	3682.057	3667.105 - 3828.552
Hydroxyl group, H-bonded, O-H stretch	- 3417.071	3592.012

3.2 Optimization Results

The responses of iron adsorption using carbonized cassava are presented in Table 3.3. It was observed from the table that the adsorption of iron on carbonized cassava is achievable because of high percentage removal.

Table 3.3: The CCRD design with response for Iron adsorption on cassava bagasse

STD	RUN	A Time(min)	B Temp.(°C)	C pH	D Dosage(g)	E Initial Conc.(ppm)	Response (% R)
42	1	65.0	60.0	7.5	0.2	201.7	98.0
40	2	65.0	60.0	7.5	0.4	112.5	79.0
33	3	5.5	60.0	7.5	0.2	112.5	60.0
35	4	65.0	36.2	7.5	0.2	112.5	97.0
41	5	65.0	60.0	7.5	0.2	23.3	97.0
43	6	65.0	60.0	7.5	0.2	112.5	93.1
48	7	65.0	60.0	7.5	0.2	112.5	93.1
19	8	40.0	70.0	5.0	0.1	150.0	75.0
10	9	90.0	50.0	5.0	0.3	75.0	93.3
39	10	65.0	60.0	7.5	0.0	112.5	0.0
24	11	90.0	70.0	10.0	0.1	150.0	76.0
13	12	40.0	50.0	10.0	0.3	75.0	79.9
44	13	65.0	60.0	7.5	0.2	112.5	93.2
22	14	90.0	50.0	10.0	0.1	150.0	80.0
32	15	90.0	70.0	10.0	0.3	150.0	93.0
26	16	90.0	50.0	5.0	0.3	150.0	89.0
20	17	90.0	70.0	5.0	0.1	150.0	81.0
50	18	65.0	60.0	7.5	0.2	112.5	93.2
8	19	90.0	70.0	10.0	0.1	75.0	71.0
7	20	40.0	70.0	10.0	0.1	75.0	63.0
28	21	90.0	70.0	5.0	0.3	150.0	93.9
12	22	90.0	70.0	5.0	0.3	75.0	96.0
21	23	40.0	50.0	10.0	0.1	150.0	70.0
11	24	40.0	70.0	5.0	0.3	75.0	85.0
45	25	65.0	60.0	7.5	0.2	112.5	93.2
36	26	65.0	83.8	7.5	0.2	112.5	98.0
3	27	40.0	70.0	5.0	0.1	75.0	72.0
9	28	40.0	50.0	5.0	0.3	75.0	80.0
46	29	65.0	60.0	7.5	0.2	112.5	93.3
5	30	40.0	50.0	10.0	0.1	75.0	66.0
17	31	40.0	50.0	5.0	0.1	150.0	70.0
23	32	40.0	70.0	10.0	0.1	150.0	67.0
18	33	90.0	50.0	5.0	0.1	150.0	80.0
38	34	65.0	60.0	13.4	0.2	112.5	56.0
6	35	90.0	50.0	10.0	0.1	75.0	77.0
16	36	90.0	70.0	10.0	0.3	75.0	93.5
31	37	40.0	70.0	10.0	0.3	150.0	81.3
1	38	40.0	50.0	5.0	0.1	75.0	70.0
15	39	40.0	70.0	10.0	0.3	75.0	80.0
25	40	40.0	50.0	5.0	0.3	150.0	77.0
49	41	65.0	60.0	7.5	0.2	112.5	93.2
47	42	65.0	60.0	7.5	0.2	112.5	93.2
37	43	65.0	60.0	1.6	0.2	112.5	61.0
27	44	40.0	70.0	5.0	0.3	150.0	84.0

2	45	90.0	50.0	5.0	0.1	75.0	81.0
30	46	90.0	50.0	10.0	0.3	150.0	95.0
29	47	40.0	50.0	10.0	0.3	150.0	80.0
4	48	90.0	70.0	5.0	0.1	75.0	80.0
34	49	124.5	60.0	7.5	0.2	112.5	87.0
14	50	90.0	50.0	10.0	0.3	75.0	95.0

Table 3.4: The ANOVA table for iron adsorption on cassava bagasse

Source	Sum of Squares	DF	Mean Square	F Value	Prob> F	
Model	7035.409	20	351.7704	646.8598	< 0.0001	Significant
A	1316.022	1	1316.022	2419.993	< 0.0001	
B	2.748927	1	2.748927	5.054917	0.0323	
C	61.21465	1	61.21465	112.5657	< 0.0001	
D	1949.08	1	1949.08	3584.102	< 0.0001	
E	3.312633	1	3.312633	6.091498	0.0197	
A^2	631.4024	1	631.4024	1161.066	< 0.0001	
B^2	43.32605	1	43.32605	79.67093	< 0.0001	
C^2	2020.184	1	2020.184	3714.854	< 0.0001	
D^2	1254.263	1	1254.263	2306.426	< 0.0001	
E^2	43.32605	1	43.32605	79.67093	< 0.0001	
AB	13.005	1	13.005	23.91449	< 0.0001	
AC	4.5	1	4.5	8.274911	0.0075	
AD	25.44222	1	25.44222	46.78492	< 0.0001	
AE	1.680556	1	1.680556	3.090322	0.0893	
BC	62.34722	1	62.34722	114.6484	< 0.0001	
BD	22.00056	1	22.00056	40.45614	< 0.0001	
BE	4.5	1	4.5	8.274911	0.0075	
CD	46.08	1	46.08	84.73509	< 0.0001	
CE	18.605	1	18.605	34.21216	< 0.0001	
DE	25.205	1	25.205	46.34869	< 0.0001	
Residual	15.77056	29	0.543813			
Lack of Fit	15.7113	22	0.71415	84.35899	< 0.0001	Significant
Pure Error	0.059259	7	0.008466			
Cor Total	7051.179	49				
Std. Dev.	0.737436		**R-Squared**	0.997763		
Mean	82.18711		**Adj R-Squared**	0.996221		
C.V.	8.9		**Pred R-Squared**	0.991543		
PRESS	59.63191		**Adeq Precision**	88.89737		

From the ANOVA (Table 3.4), the model and process parameters investigated were significant with their p-values < 0.05. The quadratic models were adequate for the experimental data based on the probability (p) value. The p-value of the model was < 0.0001 which means there was only 0.01% chance that the F-value given in the ANOVA table could occur due to noise. The predicted, actual and real coefficients of determination R^2 values were close to 1 which means that the data fit the quadratic model and suggest an excellent correlation between the independent variables. Guan and Yao (2008) reported that R^2 should be at least 0.80 for the good fit of a model. A relatively low value of coefficient of variation (CV = 8.9%) indicates a good precision and reliability of the experiments carried out.

3.3 Interactive effects of process parameters on percentage removal of iron

The 3D plots of the parameters are shown in Figures 3.1 to 3.9 for iron adsorption on cassava bagasse. The interactive effects of time and temperature on percentage removal of iron for carbonized cassava is shown in Figure 3.1 below. From the figure, it could be observed

that percentage removal increased as both time and temperature increased. The interaction between time and temperature was significant as shown in Table 3.4 above.

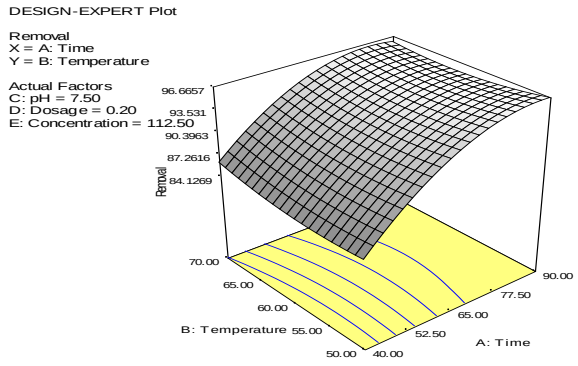

Fig 3.1: the 3D plot of time, temperature and % R for Iron adsorption on cassava bagasse

The interactive effects of time and pH on percentage removal of iron for carbonized cassava is shown in Figure 3.2 below. From the figure, it could be observed that percentage removal increased as time increased and as pH decreased. Time and pH interaction has significant interaction on percentage removal of iron using carbonized cassava bagasse.

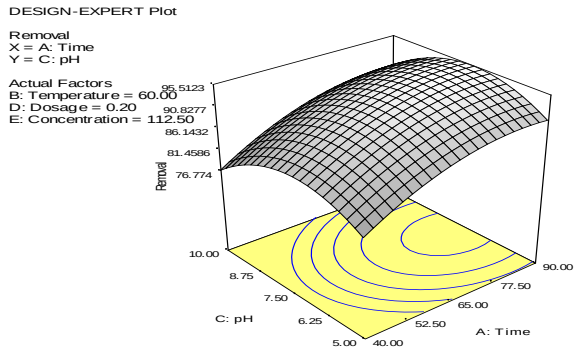

Fig 3.2: the 3D plot of time, pH and % R for iron adsorption on cassava bagasse

The interactive effects of time and dosage on percentage removal of iron carbonized cassava The interactive effects of temperature and dosage on percentage removal of iron for carbonized cassava bagasse is shown in Figure3.5 below. From the figure, it could be observed that percentage removal increased as both temperature and dosage increased. Temperature and dosage interaction has significant interaction on percentage removal of iron.

bagasse is shown in figure 3.3 below. From the figure, it could be observed that percentage removal increased as both time and dosage increased. Time and dosage have significant interaction on percentage removal of iron.

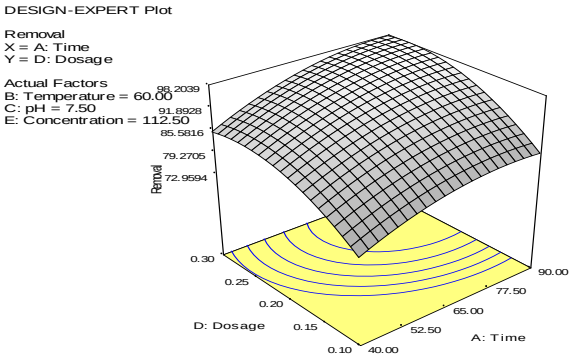

Fig 3.3: the 3D plot of time, dosage and % R for iron adsorption on cassava bagasse

The interactive effects of temperature and pH on percentage removal of iron for carbonized cassava bagasse is shown in figure 3.4 below. From the figure, it is observed that percentage removal increased as temperature increased and pH decreased. Temperature and pH interaction has significant interaction on percentage removal of iron.

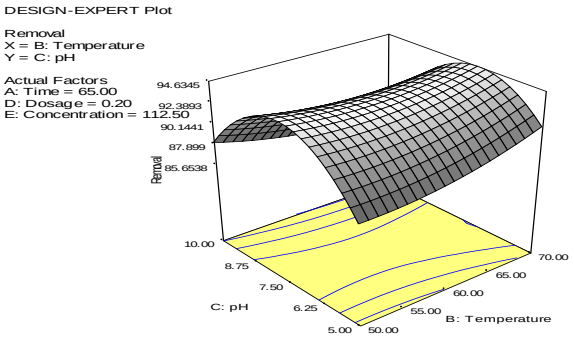

Fig 3.4: the 3D plot of temperature, pH and % R for iron adsorption on cassava bagasse

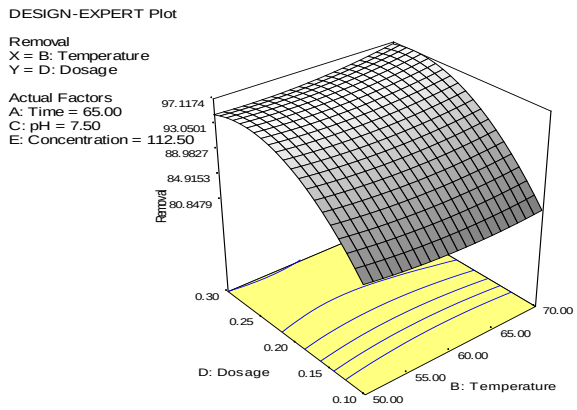

Fig 3.5: the 3D plot of temperature, dosage and %R for iron adsorption on cassava bagasse

The interactive effects of temperature and concentration on percentage removal of iron for carbonized cassava is shown in Figure3.6.From the figures, it could be observed that percentage removal increased as both temperature and concentration increased. Temperature and concentration interaction has significant interaction on percentage removal of iron.

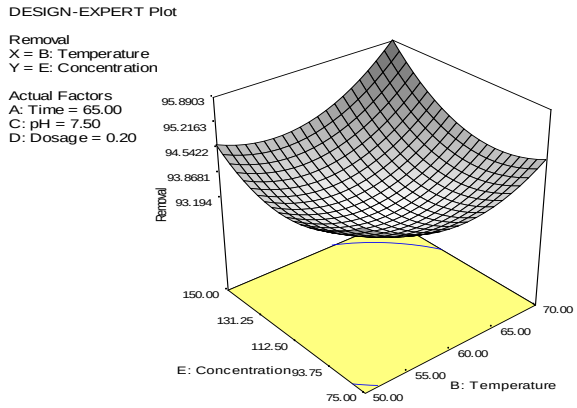

Fig 3.6: the 3D plot of temperature, concentration and % R for iron adsorption on cassava bagasse

The interaction of dosage and pH is depicted in Figure 3.7 for carbonized cassava. From the figures, it could be observed that percentage removal increased as dosage increased and pH decreased. Dosage and pH interaction has significant interaction on percentage removal of iron.

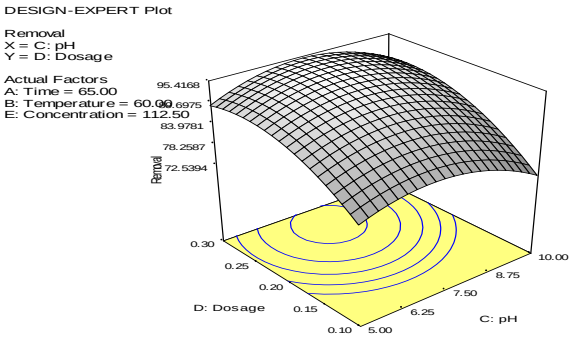

Fig 4.32: the 3D plot of dosage, pH and % R for iron adsorption on cassava bagasse

The 3D graph of Figure3.8 shows the interaction of pH and concentration against percentage removal for carbonized cassava bagasse. From the figures, it could be observed that percentage removal increased as concentration increased and pH decreased. Concentration and pH does not have significant interaction on percentage removal of iron

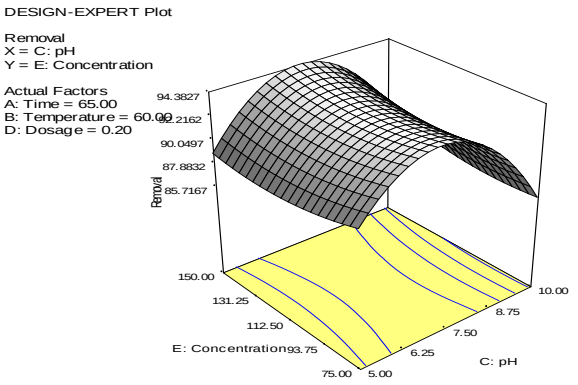

Fig 3.8: the 3D plot of concentration, pH and % R for iron adsorption on cassava bagasse

The interaction of dosage and concentration at 0.05 significance level is shown in 3D plots of Figure 3.9. From the figures, it could be observed that percentage removal increased as both dosage and concentration increased. Dosage and concentration interaction has significant interaction on percentage removal of iron.

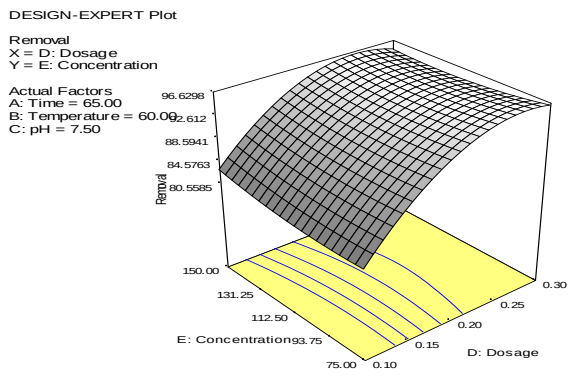

Fig 3.9: the 3D plot of concentration, dosage and % R for iron adsorption on cassava bagasse

3.4 The Model Equation

The quadratic model equations in coded and actual values are given in Equations 3.1 and 3.2. Only the non-significant term (AE) was dropped out of Equation 3.2. Among the main factors in equation 3.2, only temperature and concentration have negative coefficients; time, pH and dosage have positive coefficients. Increasing the factors with positive coefficient would increase the response and decreasing the factors with negative coefficient would decrease the response. Among the 2-factor interactions, time-temperature, pH-temperature, and dosage-concentration have negative coefficients, other interactions have positive coefficient. When other factors are held constant, two factors whose interaction have positive coefficient must head towards the same direction in order to have increase in the response. On the other hand, two factors whose interaction has negative coefficient must head towards opposite direction in order to have increase in response.

Removal (Y) = +93.23+ 5.51 *A+ 0.25*B- 1.19 *C+ 6.89*D+ 0.28*E-3.36*A^2+ 0.88*B^2- 6.01* C^2- 5.39 *D^2+ 0.88*E^2- 0.64*A *B+ 0.37*A*C+ 0.89*A*D- 0.23*A*E- 1.40* B*C+ 0.83*B*D + 0.37*B*E + 1.20 *C*D+0.76 *C*E - 0.89 *D*E **(3.1)**

3.5: Numerical Optimum Solution for Iron Adsorption

The numerical optimum solutions for iron adsorption on cassava bagasse are 86minutes, 64˚C, 7.47, 0.2g/30 ml, 139mg/l and 97.4% for time, temperature, pH, dosage, concentration and percentage removal respectively. The numerical solutions were verified by carrying out adsorption process at the given optimum points and the actual percentage removal are as shown in Tables 3.5.

Table 3.5: Numerical optimum solutions for iron adsorption

Adsorbent	Time (min)	Temp. (˚C)	pH	Dosage (g/30mL)	Conc. (mg/L)	Removal (%)	Actual % R	% Error
Cassava bagasse	86.14	64.65	7.47	0.24	139.35	98.23	96.8	1.48

ACKNOWLEDGEMENT

The authors send many thanks to Chemical Engineering Laboratory, Enugu State University of Science and Technology (ESUT), Enugu and Project Development Institute (PRODA), Enugu for the use of their facilities.

REFERENCES

AOAC (1990). Official Method of Analysis. 15th Edition, AOAC, Association of Official Analytical Chemists, Washington, DC.

Gassan, H., Ochando, P., Saloua, B.D., & Rodriguez-Vives, A. (2013). Kinetics and Thermodynamic Parameters of Iron Adsorption onto Olive Stones. *Journal of Industrial Crops and Products, 49,* 526-534.

Guan, X, Yao, H. (2008). Optimization of Viscoenzyme L-assisted extraction of oat bran protein using response surface methodology. Food Chemistry, 106, 345-351.

Gupta, V.K., Nayak A., &Agarwal S., (2015). Bioadsorbents for remediation of heavy metals,

current status and their future prospects. *Environment-Engineering Research, 20,* 01-018.

Osvaldo Karnitz, et al. (2007). Adsorption of heavy metal ion from aqueous single metal solution by chemically modified sugarcane bagasse. *Bioresource Technology, 98 (*6) 1291–1297.

Sarkar, M., Acharya, P.K., &Battacharya, B. (2003). Modeling the adsorption kinetics of some priority organic pollutants in water from diffusion and activation energy parameters. *Journal of Colloid Interface Science, 266,* (1), 28-32.

Tamer, M., Alslaibi, Ismail A., MohdAzmier A., & Abu F., (2013). Cadmium removal from aqueous solution using microwaved olive stone activated carbon. *Journal of Environmental Chemical Engineering 1(3),* 589-599.

Trueby, P. (2003). Impact of heavy metals on forest trees from mining areas. In: International Conference on Mining and the Environment III, Sudbury, Ontario, Canada.

United Nations Commission for Sustainable Development (CSD-18), (2010). Hazardous Waste Interactive Discussions and Ministerial Round Table on Waste Management.

Urbain, K., Aime S.E., Jacques, A.Y., & Albert, T. (2013). Adsorption of Iron and Zinc on Commercially Activated Carbon. *Journal of Environmental Chemistry and Ecotoxicology; 5(6),* 168-171.